Qualitative modeling of the dynamics of detonations with losses

Luiz M. Faria and Aslan R. Kasimov

Applied Mathematics and Computational Science
Room 4-2226, 4700 King Abdullah University of Science and Technology
Thuwal 23955-6900, Saudi Arabia

arXiv:1407.8475v1 [physics.flu-dyn] 31 Jul 2014

Abstract

We consider a simplified model for the dynamics of one-dimensional detonations with generic losses. It consists of a single partial differential equation that reproduces, at a qualitative level, the essential properties of unsteady detonation waves, including pulsating and chaotic solutions. In particular, we investigate the effects of shock curvature and friction losses on detonation dynamics. To calculate steady-state solutions, a novel approach to solving the detonation eigenvalue problem is introduced that avoids the well-known numerical difficulties associated with the presence of a sonic point. By using unsteady numerical simulations of the simplified model, we also explore the nonlinear stability of steady-state or quasi-steady solutions.

Keywords: Detonation theory, non-ideal detonation, detonation initiation/failure, detonation with friction, curvature effects

1. Introduction

A gaseous detonation is a phenomenon exhibiting rich dynamical features. One-dimensional planar detonations propagate with a velocity that can be steady, periodic, or chaotic [1]. In multiple dimensions, the detonation front includes complex structures resulting in cellular patterns formed by triple-point trajectories [2, 3]. Quasi-steady curved detonations, characteristic of condensed explosives, possess multiple-valued solutions at a given curvature [4]. The same multiplicity of solutions exists in one-dimensional detonations in the presence of heat and momentum losses [5, 6, 7, 8]. This range of complex dynamical properties of detonations poses a challenge in terms of theoretical understanding of conditions in which they arise and of features they exhibit. The linear stability theory for idealized

Email address: aslan.kasimov@kaust.edu.sa (Luiz M. Faria and Aslan R. Kasimov)

systems, asymptotic theories of weakly curved detonation, and other asymptotic models have significantly advanced our understanding of the detonation phenomenon (see recent reviews in [9]). However, many problems still require further theoretical study, including the mechanism of detonation cell formation, the nature of critical conditions of detonation propagation in systems with losses, the linear and nonlinear instability in systems described by complex reactions and equations of state, and others.

Elucidation of key physical mechanisms of the complex phenomena of detonation dynamics is greatly facilitated by simplified models, including those of *ad hoc* nature [10]. Such models can highlight in the clearest possible way the processes responsible for a particular qualitative trait in the observed dynamics. A wide range of dynamical properties of one-dimensional detonations, including chaotic solutions, is reproduced in [11, 12] with a simple extension of Fickett's analog [10] to model the chemical reaction with a well-defined induction zone followed by a heat-release zone. In [13, 14], it was shown that a model consisting of just a single scalar equation is also capable of qualitatively capturing the dynamics of one-dimensional detonations in the reactive Euler equations, including instability and chaos. The most important implication of these simplified models is that the true nature of the complex dynamics of detonations appears to be governed by a simple mechanism, thus providing a strong indication that a rational reduction of the reactive Euler equations that retains the same essential physical ingredients as the simple models may be feasible.

The model in [13] is given by the following equation:

$$\frac{\partial u}{\partial t}+\frac{\partial}{\partial x}\left(\frac{u^2}{2}-\frac{uu_s}{2}\right)=f\left(x,u_s\right), \tag{1}$$

where $x\leq 0$ is the reaction zone behind the shock propagating from left to right. Equation (1) is written in a shock-attached frame; the shock location is hence at $x=0$ at all times, t. The unknown, $u\left(x,t\right)$, plays the role of, e.g., pressure, while u_s is the solution u evaluated at the shock, and it is related to the shock speed through shock conditions. The forcing function, f, is chosen to mimic the behavior of the reaction rate in the reactive Euler equations. In particular, it is taken to have a maximum at some distance away from the shock, $x_f=x_f\left(u_s\right)$, with function x_f chosen to depend sensitively on the shock state, u_s. The following choice,

$$f=\frac{a}{\sqrt{4\pi\beta}}\exp\left[-\frac{\left(x+u_s^{-\alpha}\right)^2}{4\beta}\right], \tag{2}$$

where $a=\left[4\left(1+\mathrm{erf}\left(u_s^{-\alpha}/2\sqrt{\beta}\right)\right)\right]^{-1}$, is used in numerical calculations below, as in [14]. In this form, the model is

dimensionless with u scaled so that $u_s = 1$ in the steady state. Parameters α and β are analogous to the activation energy in the reactive Euler equations with Arrhenius kinetics and to the ratio of the reaction-zone length to the induction-zone length, respectively. Note that the total chemical energy released corresponds to $\int_{-\infty}^{0} f(x, u_s(t))dx$, which is constant for the forcing term (2) regardless of the value of $u_s(t)$. This follows from $f \sim \lambda_x$, as discussed in [13, 14]. Thus, the total energy released is always the same even in the presence of instabilities.

Equation (1) can be shown to be closely related to the asymptotic model [15] derived from the reactive Euler equations. From a physical point of view, an important ingredient of the model is that it represents the nonlinear interaction of two wave families: one moving slowly toward the shock and one moving infinitely quickly away from the shock. The former is simply the wave evolving along the Burgers characteristic. The wave moving infinitely fast is implied by the presence of the shock state, u_s, directly in (1), such that the solution, $u\,(x,t)$, at any given time, t, at any location, x, depends on the shock state at that particular time. This non-locality is a result of taking to an extreme the asymptotic idea that the waves reflecting from the shock propagate much faster than the waves moving toward the shock from the reaction zone. Another element of the model that is of physical significance is that when f has a maximum at some distance away from the shock, and the position of this maximum depends sensitively on the shock state, the system represents a kind of a resonator that amplifies the waves moving back and forth between the shock and the region around x_f. This resonant amplification is a real mechanism for instability as observed in the simulations of pulsating solutions of (1) [14].

2. A model with generic losses

Our focus here is to explore the effect of generic losses on the solutions of (1). For this purpose, we modify the forcing in (1) to add a damping term,

$$\frac{\partial u}{\partial t} + \frac{\partial}{\partial x}\left(\frac{1}{2}u^2 - Du\right) = f\,(x, D) - g(x, u, \varphi). \tag{3}$$

Here, $D = u_s/2$ is the detonation speed, which is obtained using the Rankine-Hugoniot conditions with the state upstream of the shock taken to be $u = 0$ [14], φ is a parameter of the problem, which may be time dependent, and g is a function that represents the loss. Friction losses are modeled by taking $g = c_f u|u|$, with the friction coefficient c_f, while the effects of curvature are modeled by taking $g = \kappa u^2/\,(1 + \kappa x)$, where κ is the shock curvature, generally dependent on time.

2.1. Steady and quasi-steady solutions

If φ is a constant, then we can find steady-state solutions of (3). If φ is time-dependent, but slowly varying in time, then we can find quasi-steady solutions of (3). In both cases, the problem requires solving the ordinary differential equation (ODE),

$$(u - D)\, u' = f\,(x, D) - g(x, u, \varphi), \tag{4}$$

on $x \in [a, 0]$ with $u(0) = 2D$ as the shock condition. Here and below, primes denote the derivative, d/dx. The left end of the integration region is either $a = -\infty$ or the sonic locus, $a = x_*$, where $u - D = 0$. The main problem is to determine the detonation speed, D, such that the corresponding solution, $u\,(x, t)$, of (4) is a smooth function of x. This is a nonlinear eigenvalue problem for D because such smooth solutions do not necessarily exist for every D at a given φ. For physically interesting choices of f and g, there usually exists a sonic point where $u = D$, which is a singular point of (4). For smoothness of u, it is necessary that the right-hand side of (4) vanishes at the sonic point. These conditions constitute the generalized Chapman-Jouguet conditions of detonation theory and serve to determine the eigenvalue relation, $H(D, \varphi) = 0$, that yields D for a given φ. Typically, $D\,(\varphi)$ is a multiple-valued function having a turning-point shape.

The nonlinear ODE (4) cannot, in general, be solved analytically. Therefore, a numerical integration method is required. In one such method, for a trial value of D, (4) is integrated from $x = 0$ toward $x = a$. The correct value of D has to correspond to $u - D = 0$ and $f - g = 0$ at $x = x_*$. These conditions are not satisfied in most cases, and, therefore, equation (4) is very stiff as $u \to D$, making the numerical integration prohibitively expensive and/or inaccurate. As an alternative to this method, the sonic locus, $x_*(D, \varphi)$, is found first for a trial value of D. Then, the solution of (4) is found analytically in the neighborhood of x_* in order to get out of the sonic point by a small step to $x_* + \Delta x$, with a subsequent numerical integration from $x_* + \Delta x$ toward the shock. For the correct value of D, the Rankine-Hugoniot conditions at $x = 0$ must be satisfied. This algorithm is more robust numerically. However, its drawback is that it requires the knowledge of the sonic state and the ability to solve the equation (or the system of equations, in general) in the neighborhood of the sonic locus analytically. Even though, in our case, it is straightforward to do so, in more complicated problems, this approach is not feasible [8].

Here, we propose a different algorithm that is much simpler, more robust, and easier to generalize (see Appendix for the general version of the algorithm). The key idea of the method is a change of the dependent variable that eliminates the singularity from the governing ODE. Specifically, we introduce $z = (u - D)^2$ as a new variable instead

of u. Then, (4) becomes

$$z' = 2\left(f\left(x, D\right) - g(x, u, \varphi)\right), \tag{5}$$

which has a regular right-hand side. Notice that the inverse of the transformation from u to z is double-valued, $u = D \pm \sqrt{z}$. At the shock, $u(0) = 2D > D$, and, therefore, between the shock and the sonic point, we have $u = D + \sqrt{z}$. Hence

$$z' = 2\left(f\left(x, D\right) - g(x, D + \sqrt{z}, \varphi)\right). \tag{6}$$

Downstream of the sonic point, the square root changes its branch. Therefore, $u = D - \sqrt{z}$. The sonic condition in the new variable is very simple: $z' = 0$ at $z = 0$. These conditions are clearly independent of the specific form of the right-hand side of (4). The main advantages of the new algorithm are that the equations are no longer stiff and that the sonic conditions are very simple. If the solution beyond the sonic point is required, then $z' = 2\left(f\left(x, D\right) - g(x, D - \sqrt{z}, \varphi)\right)$ must be solved at $x < x_*$.

The substitution employed here is applicable to a wide range of problems [8]. For example, the problem of finding a quasi-steady solution of a curved expanding detonation leads to the ODE for the flow velocity (e.g., [4]):

$$\frac{du}{d\lambda} = \frac{\Phi}{u^2 - c^2}\frac{u}{\omega}, \tag{7}$$

where $\omega = k\left(1 - \lambda\right)\exp(-\gamma\vartheta/c^2)$ is the reaction rate, ϑ is the activation energy, $\Phi = \left(\gamma - 1\right)q\omega - \kappa c^2\left(u + D\right)$, κ is the shock curvature, q is the heat release, and $c^2 = \gamma p_0 + \left(\gamma - 1\right)\left[\left(D^2 - u^2\right)/2 + q\lambda\right]$. The integration domain is $0 \le \lambda \le 1$ with $u(0) = u_s(D)$ given by the Rankine-Hugoniot condition. The sonic singularity here occurs at $u = c$ and hence we introduce $z = \left(u - c\right)^2$ to obtain

$$\frac{dz}{d\lambda} = 2\left(u - c\right)\left(1 - \frac{\partial c}{\partial u}\right)\frac{du}{d\lambda} = 2\left(1 - \frac{\partial c}{\partial u}\right)\frac{\Phi u}{\omega}, \tag{8}$$

which is regular at the sonic point. After the correct branch of the inversion is obtained, the generalized Chapman-Jouguet condition at the sonic point in terms of the new variables is that $dz/d\lambda = 0$ at the sonic point, $\lambda = \lambda^*$, where $z(\lambda^*) = 0$. This provides a much simpler and faster way of solving the generalized Chapman-Jouguet condition and allows for integration from the shock toward the sonic point without any difficulty.

2.2. On linear stability analysis

Once the steady or quasi-steady solutions are obtained, the question of their linear stability arises. The problem without losses is analyzed extensively in [14], where it is shown that the analysis parallels that of the reactive Euler equations.

We begin with the stability of steady-state solutions. Let $u_0(x)$ be the solution of

$$\frac{d}{dx}\left(\frac{1}{2}u_0^2 - D_0 u_0\right) = f\left(x, D_0\right) - g(x, u_0, \varphi), \tag{9}$$

where φ is a constant and D_0 is such that the generalized Chapman-Jouguet condition is satisfied. Consider then a perturbation of this solution of the form $D = D_0 + \epsilon\sigma \exp(\sigma t)$ and $u = u_0(x) + \epsilon u_1(x)\exp(\sigma t)$, where σ is the growth rate to be found. Inserting these expansions into (3) yields

$$\sigma u_1 + \left(u_0 u_1 - D_0 u_1 - \sigma u_0\right)' \quad = \quad \sigma \frac{\partial f}{\partial D}\left(x, D_0\right) - u_1 \frac{\partial g}{\partial u}(x, u_0, \varphi), \tag{10}$$

which can be solved exactly to yield the eigenfunction,

$$u_1\left(x\right) = \frac{\sigma}{c_0(x)} e^{p(x,\sigma)} \left[\int_0^x \left(\frac{\partial f}{\partial D}\left(x, D_0\right) + u_0'\right) e^{-p(\xi,\sigma)} d\xi + 2D_0\right],$$

where $c_0 = u_0 - D_0$ and

$$p(x,\sigma) = \int_x^0 \left[\sigma + \frac{\partial g}{\partial u}(\xi, u_0(\xi), \varphi)\right] \frac{d\xi}{c_0(\xi)}$$

are functions of f and g, which are known in terms the steady-state solution, $u_0\left(x\right)$. Requiring boundedness of the eigenfunctions gives the dispersion relation

$$\int_{x_*}^0 \left(\frac{\partial f}{\partial D}\left(\xi, D_0\right) + u_0'\right) e^{-p(\xi,\sigma)} d\xi - 2D_0 = 0, \tag{11}$$

which is the same as in the ideal case with the only change due to g appearing in the expression for p. Hence, the stability analysis of the equation with losses is very similar to the ideal case analyzed in [14].

For quasi-steady problems, the stability analysis is a bit subtler. Consider

$$\frac{\partial u}{\partial t} + \frac{\partial}{\partial x}\left(\frac{1}{2}u^2 - Du\right) = f\left(x, D\right) - g(x, u, \varphi), \tag{12}$$

where φ is a slowly varying function of time. Then, the steady-state solution for u does not exist in general. We then consider solutions that are slowly evolving in time by considering a slow time variable, $\tau = \delta t$, $0 < \delta \ll 1$, such

that $\varphi = \varphi(\tau)$. Then,

$$\delta \frac{\partial u}{\partial \tau} + \frac{\partial}{\partial x}\left(\frac{1}{2}u^2 - Du\right) = f(x, D) - g(x, u, \varphi(\tau)). \tag{13}$$

Let $u_\delta(x, \tau)$ be the exact solution of (13) with $D = D_\delta(\tau)$ as the speed. Then, the spectral stability of this solution requires looking at the evolution of $D = D_\delta(\tau) + \epsilon\sigma \exp(\sigma t)$ and $u = u_\delta(x, \tau) + \epsilon u_{\delta 1}(x, \tau)\exp(\sigma t)$. It is important to observe that these expansions express $O(1)$ time-scale variations around the slow, $O(1/\delta)$, time-scale leading solution. Putting these expressions into (13), we obtain, to first order,

$$\delta \frac{\partial u_{\delta 1}}{\partial \tau} + \sigma u_{\delta 1} + \frac{\partial}{\partial x}\left(u_\delta u_{\delta 1} - D_\delta u_{\delta 1} - \sigma u_\delta\right) \quad = \tag{14}$$

$$\sigma \frac{\partial f}{\partial D}(x, D_\delta) - u_{\delta 1}\frac{\partial g}{\partial u}(x, u_\delta, \varphi). \tag{15}$$

Next, we perform an asymptotic expansion in δ: $u_\delta = u_0 + O(\delta)$, $u_{\delta 1} = u_1 + O(\delta)$, $D_\delta = D_0 + O(\delta)$. Then, to leading order, the quasi-steady solution satisfies

$$\frac{d}{dx}\left(\frac{1}{2}u_0^2 - D_0 u_0\right) = f(x, D_0) - g(x, u_0, \varphi), \tag{16}$$

which, together with the shock and sonic conditions, gives the eigenvalue problem for D_0. The linear stability equation is, to leading order in δ, given by the same equation as (10) and hence the dispersion relation is also given by (11). Notice here that the implicit assumption $\partial u_0/\partial \tau = O(1)$ is required for the validity of the asymptotic expansion in δ. This is seen to break down at a turning point of the $D_0 - \varphi$ curve if such a point exists.

3. Numerical results

In this section, we investigate numerically two types of losses, frictional and those due to shock curvature. For detonation with frictional losses, we consider

$$\frac{\partial u}{\partial t} + \frac{\partial}{\partial x}\left(\frac{1}{2}u^2 - Du\right) = f(x, D) - c_f u|u|, \tag{17}$$

where $x \in (-\infty, 0]$ and c_f is a constant friction coefficient. The goal of the following calculations is to determine the role of c_f in the existence and structure of the steady-state solutions of (17). Figure 1 shows the computed dependence of $u_s = 2D$ on c_f, where we can see the characteristic turning-point behavior with two solutions coexisting at $c_f < c_{fc}$ and steady-state solutions no longer existing if $c_f > c_{fc}$.

Of particular interest is the question of stability of these steady-state solutions. It is generally believed that

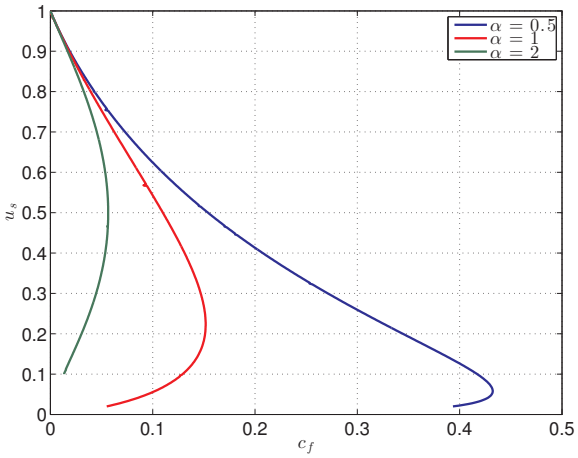

Figure 1: The $u_s - c_f$ relation for the steady-state solution of (17) for detonation with friction.

the lower branch of the steady-state u_s-c_f curve is always unstable while the top branch can be stable or unstable. In order to explore the nature of these instabilities, we solve (17) numerically using a second-order finite volume Godunov's method with a min-mod limiter [16]. We begin with a perturbation around the steady-state solutions at different locations of the u_s-c_f curve, both on the top and bottom branches. We choose α and β such that the corresponding ideal solution is stable.

We find that as we increase c_f along the top branch, there is a critical value of c_f above which the detonation becomes unstable, indicating that the losses have a destabilizing effect. Figure 2 shows the computed solutions at $c_f = 0.1$, corresponding to a stable state on the upper branch, and $c_f = 0.125$, corresponding to an unstable state on the upper branch. Note that the instability of the steady-state solutions on the top branch is associated with a transition to a limit cycle, likely arising through a Hopf bifurcation when c_f exceeds a critical value. These oscillations take place around the steady-state solution.

As we solve the problem starting on the bottom branch, we find that the steady-state solution on the branch is indeed unstable, but, unlike the solutions on the top branch, there is no oscillation around the bottom branch. The solution tends in fact toward the top branch with time, indicating that the bottom branch is generally a repelling equilibrium while the top branch is attracting. The dynamics of this instability is quite different from that on the top branch. It involves a generation of internal shock waves in the reaction zone that overtake the lead shock and, eventually, after multiple such overtakings, the solution settles on the top branch. The discontinuous behavior of

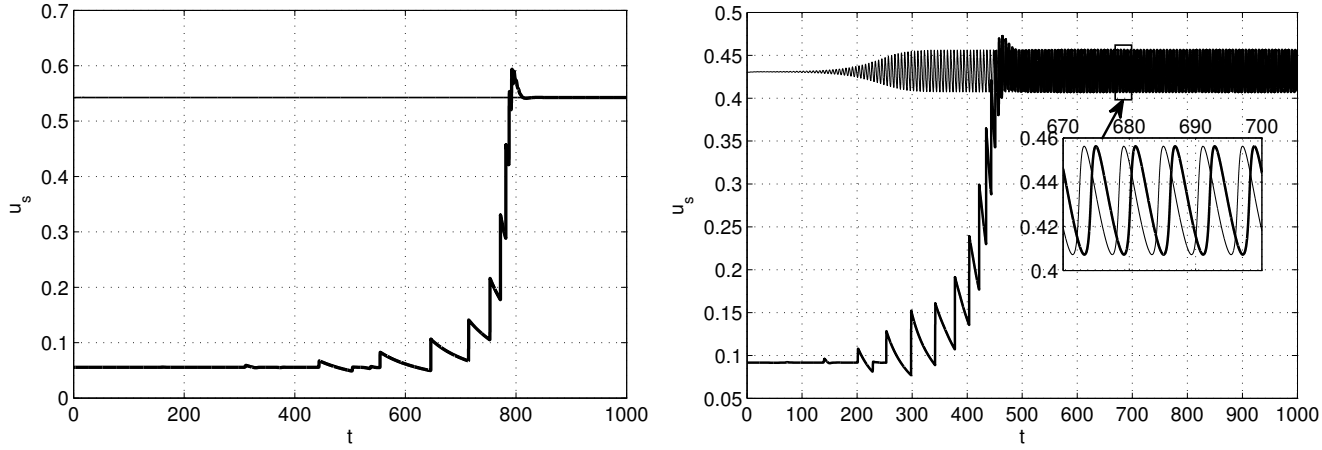

Figure 2: Time evolution of solutions for detonation with friction starting with the middle curve of Fig. 1 at $\alpha = 1$: (a) at $c_f = 0.1$, the top branch is stable, the integration is carried out starting both from the top branch (thin curve) and the bottom branch (thick curve); (b) the same, but at $c_f = 0.125$, which corresponds to unstable solutions around the top branch. The pulsating instability in (b) is due purely to the presence of friction.

the thick curves in Fig. 2 occurs precisely when an internal shock wave catches up with the lead shock. At that moment, there is a rapid increase of u_s. The general trend of the solution appears to be physically reasonable, reflecting the strong instability of the lower branch of the D-c_f curve and the attracting character of the upper branch. It is interesting that very similar behavior was observed in experiments on initiation of spherical detonation in hydrocarbon-air mixtures [17].

Now, we look at spherically expanding detonation solutions. The shock-frame version of (1) for a diverging detonation is given by

$$\frac{\partial u}{\partial t} + \frac{1}{2}\frac{\partial}{\partial x}\left(u^2 - uu_s\right) = f\left(x, u_s\right) - \frac{u^2}{x + r_s}, \tag{18}$$

where $r_s\left(t\right)$ denotes the shock radius such that $dr_s/dt = D = u_s/2$. When $\partial u/\partial t$ is dropped, (18) can be written as

$$\frac{du_0}{dx} = \frac{f\left(x, u_s\right) - \kappa u_0^2/\left(1 + \kappa x\right)}{u_0 - u_s/2}, \tag{19}$$

where $\kappa = 1/r_s$ is the mean curvature of the shock. This equation must be solved subject to $u_0\left(0\right) = u_s$ and to some appropriate condition at $x = -r_s$, i.e., at $r = 0$.

Equation (19) is solved using the algorithm described earlier. In Fig. 3(a), we show the computed dependence of u_s on κ for various values of α at $\beta = 0.1$. The usual turning-point behavior is seen with the critical curvature

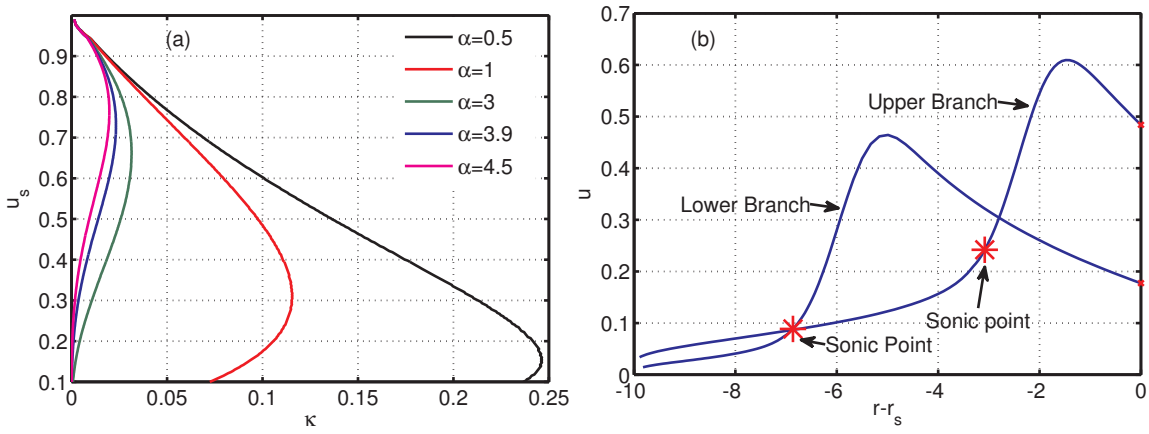

Figure 3: (a) Quasi-steady $u_s - \kappa$ curves at $\beta = 0.1$ fixed and variable α. (b) The quasi-steady solution profiles $u_0(x)$ on the top and the bottom branches of the $u_s - \kappa$ curve in (a) at $\alpha = 1$ and $\kappa = 0.1$.

decreasing as α increases. This is similar to that in the Euler detonations wherein the activation energy leads to the same effects [18, 19]. One important difference is that, in Fig. 3(a), there are only two branches, the lower branch tending to $u_s = 0$ and $\kappa = 0$, while in the Euler equations, there are in general three branches, the lower branch tending to $D = c_a$, the ambient sound speed, and $\kappa \to \infty$. In Fig. 3(b), we also show the solution profiles that correspond to the $u_s - \kappa$ curves in Fig. 3(a) at a particular value of $\kappa = 0.1$, but at two different values of u_s, one on the upper branch and one on the lower. A notable feature of these profiles is the existence of an internal maximum of u, which does not exist in the planar solution at the same parameters.

In order to understand better the role of the curvature term in (18), we solve the equation simulating the direct initiation of gaseous detonation. In the laboratory frame of reference, (18) takes the form

$$\frac{\partial u}{\partial t} + \frac{\partial}{\partial r}\left(\frac{u^2}{2}\right) = -\frac{u^2}{r} + \begin{cases} f\left(r - r_s, u\left(r_s, t\right)\right), & r < r_s, \\ 0, & r > r_s. \end{cases} \tag{20}$$

We solve this equation using a fifth-order WENO algorithm [20] and the initial conditions corresponding to a localized source of the type $u(r,0) = u_i$ at $0 < r < r_i$ and $u(r,0) = 0$ at $r > r_i$. Here, r_i is the radius of the initial hot spot and u_i is its "temperature". The point-blast initiation is simulated keeping r_i fixed at some small value and varying u_i, a measure of the source energy.

Our findings are displayed in Fig. 4. We select two sets of parameters for α and β such that one corresponds to a

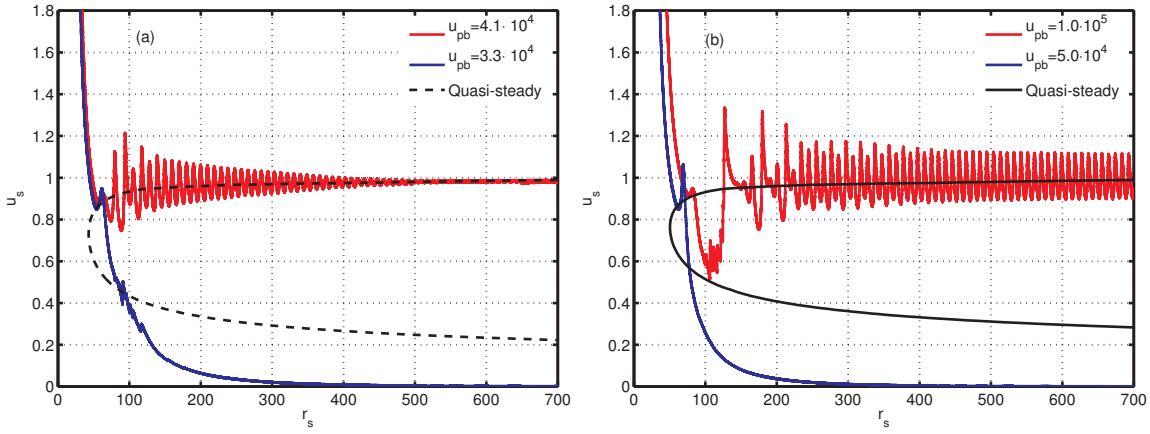

Figure 4: Initiation and failure of: (a) stable solutions at $\alpha = 3.9$ and (b) unstable solutions at $\alpha = 4.5$. In both figures, $\beta = 0.1$, the length of the computational domain is $L = 10^3$, and the number of grid points used is $N = 10^4$.

stable planar solution and the other to an unstable planar solution. For each case, we vary u_i to see if the detonation initiates or fails. Exactly as in the Euler detonations [21], we observe that above a certain critical value, u_{ic}, there is an initiation; below there is failure. Moreover, the curvature in our model also plays a destabilizing role. As one can see in Fig. 4(a), the detonation that is stable in the planar case oscillates in the presence of significant curvature. The oscillations are large in magnitude and irregular at first, around $r_s = 100$ to about $r_s = 150$, before settling down to regular decaying oscillations. A similar trend is seen in the unstable case, shown in Fig. 4(b), where the range of the irregular oscillations extends from about $r_s = 120$ to $r_s = 400$ before settling down to regular periodic oscillations. When the curvature is significantly diminished, the detonation dynamics is essentially that of a planar wave. Hence, all the phenomena observed in [13, 14] carry over to the present study. However, the destabilizing effect of curvature, clearly seen in Fig. 4, requires further analysis in order to reveal the underlying mechanisms. An additional factor that contributes to the instability of the solutions is β. For planar solutions, we have shown in [14] that smaller β leads to more unstable solutions, and we expect the same effect to be preserved in the curved detonations as well.

4. Conclusions

A reactive Burgers equation with nonlocal forcing and appropriate damping is shown to capture, at a qualitative level, the dynamics of detonations with friction and of radially diverging detonations. Using a new integration

algorithm, we have found that for curved detonations and for non-ideal detonations, steady/quasi-steady solutions exist, which have a characteristic turning-point shape in the plane of the shock speed versus curvature or a friction coefficient. Unsteady numerical simulations of our model equation reproduce the dynamics of the point-blast initiation, capturing the initiation/failure phenomenon. The curvature or the presence of friction are found to play a destabilizing role in the dynamics of non-ideal detonation. The present calculations together with our earlier study of the planar model demonstrate that the reactive Burgers equation is capable of reproducing, qualitatively, most of the dynamical properties of one-dimensional detonations.

Acknowledgements

The research reported here was supported by King Abdullah University of Science and Technology (KAUST).

References

[1] H. Ng, A. Higgins, C. Kiyanda, M. Radulescu, J. Lee, K. Bates, and N. Nikiforakis. Nonlinear dynamics and chaos analysis of one-dimensional pulsating detonations. *Combust. Theory Model*, 9(1):159–170, 2005.

[2] J. H. S. Lee. *The Detonation Phenomenon*. Cambridge University Press, 2008.

[3] W. Fickett and W. C. Davis. *Detonation: theory and experiment*. Dover Publications, 2011.

[4] J. B. Bdzil and D. S. Stewart. Theory of detonation shock dynamics. In *Shock Waves Science and Technology Library, Vol. 6*, pages 373–453. Springer, 2012.

[5] Y. B. Zel'dovich. On the theory of propagation of detonation in gaseous systems. *J. Exp. Theor. Phys.*, 10(5):542–569, 1940.

[6] Y. B. Zel'dovich and A. S. Kompaneets. *Theory of Detonation*. New York: Academic Press, 1960.

[7] I. Brailovsky, L. Kagan, and G. Sivashinsky. Combustion waves in hydraulically resisted systems. *Philosophical Transactions of the Royal Society A: Mathematical, Physical and Engineering Sciences*, 370(1960):625–646, 2012.

[8] R. Semenko, L. M. Faria, A. R. Kasimov, and B. S. Ermolaev. Set-valued solutions for non-ideal detonation. *http://arxiv.org/pdf/1312.2180v1.pdf*, 2013.

[9] F. Zhang, editor. *Shock Waves Science and Technology Library, Vol. 6: Detonation Dynamics*. Springer, 2012.

[10] W. Fickett. Detonation in miniature. *American Journal of Physics*, 47(12):1050–1059, 1979.

[11] M. I. Radulescu and J. Tang. Nonlinear dynamics of self-sustained supersonic reaction waves: Fickett's detonation analogue. *Phys. Rev. Lett.*, 107(16), 2011.

[12] J. Tang and M.I. Radulescu. Dynamics of shock induced ignition in Ficketts model: Influence of χ. *Proceedings of the Combustion Institute*, 2012.

[13] A. R. Kasimov, L. M. Faria, and R. R. Rosales. Model for shock wave chaos. *Physical Review Letters*, 110(10):104104, 2013.

[14] L. M. Faria, A. R. Kasimov, and R. R. Rosales. Study of a model equation in detonation theory. *SIAM Journal on Applied Mathematics*, 74(2):547–570, 2014.

[15] R. R. Rosales and A. J. Majda. Weakly nonlinear detonation waves. *SIAM Journal on Applied Mathematics*, 43(5):1086–1118, 1983.

[16] R. J. LeVeque. *Finite volume methods for hyperbolic problems*. Cambridge University Press, 2002.

[17] D. C. Bull, J. E. Elsworth, and G. Hooper. Initiation of spherical detonation in hydrocarbon/air mixtures. *Acta Astronautica*, 5(11):997–1008, 1978.

[18] J. B. Bdzil and D. S. Stewart. The dynamics of detonation in explosive systems. *Ann. Rev. Fluid Mech.*, 39:263–292, 2007.

[19] A. R. Kasimov and D. S. Stewart. Asymptotic theory of evolution and failure of self-sustained detonations. *J. Fluid Mech.*, 525:161–192, 2005.

[20] A. K. Henrick, T. D. Aslam, and J. M. Powers. Simulations of pulsating one-dimensional detonations with true fifth order accuracy. *J. Comput. Phys.*, 213(1):311–329, 2006.

[21] S.D. Watt and G.J. Sharpe. Linear and nonlinear dynamics of cylindrically and spherically expanding detonation waves. *Journal of Fluid Mechanics*, 522(1):329–356, 2005.

[22] A. J. Higgins. Steady one-dimensional detonations. In *Shock Waves Science and Technology Library, Vol. 6*, pages 33–105. Springer, 2012.

[23] M.R. Flynn, A. R. Kasimov, J.-C. Nave, R.R. Rosales, and B. Seibold. Self-sustained nonlinear waves in traffic flow. *Phys. Rev. E*, 79(056113), 2009.

[24] R. Klein and D. S. Stewart. The relation between curvature, rate state-dependence, and detonation velocity. *SIAM Journal on Applied Mathematics*, 53(5):1401–1435, 1993.

Appendix A. Transonic integration of reactive Euler equations

Here, we describe an algorithm for numerical integration of the system of ordinary differential equations (ODE) for the transonic structure of traveling-wave solutions of reactive Euler equations in one spatial dimension. Because the algorithm works for a general one-dimensional system of hyperbolic balance laws, we begin with such a system. Then we specialize to a system of reactive Euler equations and provide an example of a weakly curved detonation.

Consider a system of hyperbolic balance laws,

$$\boldsymbol{q}_t + \mathbf{F}(\boldsymbol{q})_x = \mathbf{s}\left(\mathbf{q}\right), \tag{A.1}$$

where $\mathbf{q}$ is the vector of unknowns, $\mathbf{F}$ is the flux vector, and $\mathbf{s}$ is a source term. We look for traveling wave solutions $\boldsymbol{q} = \boldsymbol{q}(x - Dt) = \boldsymbol{q}(\eta)$, consisting of a shock followed by a smooth flow downstream. The state upstream of the shock, $\eta > 0$, is assumed to be uniform and steady, $\boldsymbol{q} = \boldsymbol{q}_a = constant$. Then, $\mathbf{q}$, solves

$$\left(\mathbf{F}(\boldsymbol{q}) - D\boldsymbol{q}\right)_\eta = \mathbf{s} \tag{A.2}$$

in smooth parts of the flow, where $\eta = 0$ is the shock position and $\eta < 0$ is the downstream region. At $\eta = 0$, the following shock conditions are satisfied:

$$-D\left[\mathbf{q}\right] + \left[\mathbf{F}\right] = 0, \tag{A.3}$$

with $[Z] = Z^+ - Z^-$ denoting the jump in the quantity Z across the shock. The solution of (A.3) can be written as $\boldsymbol{q}(0_-) = \boldsymbol{q}_{RH}(D, \boldsymbol{q}_a)$. The shock speed, D, is an unknown of the problem and must be found together with the profiles of $\mathbf{q}$ at $\eta < 0$.

A well-known difficulty in solving (A.2) arises when one of the eigenvalues of the matrix, $\mathbf{F_q} - D\mathbf{I}$, where $\mathbf{F_q} \equiv \partial\mathbf{F}/\partial\boldsymbol{q}$, vanishes at some point $\eta_* < 0$ (a sonic point), thus producing a singular system of ODE, $(\mathbf{F_q} - D\mathbf{I})\,\mathbf{u}_\eta = \mathbf{s}$ [22]. This feature is an essential ingredient of any self-sustained shock wave and is thus relevant in many applications where such traveling shock-wave solutions arise (e.g., traffic flow problems [23], hydraulic jumps [**?**]). Should there be a vanishing eigenvalue, a regularity condition is called upon where, for boundedness of $\boldsymbol{q}_\eta$, it is required that

$$\mathbf{l}_* \cdot \mathbf{s}_* = 0 \quad \text{when} \quad \lambda_* = 0, \tag{A.4}$$

where λ_* is the special eigenvalue of $\mathbf{F_q} - D\mathbf{I}$ that vanishes at η_* and $\mathbf{l}_*$ is the corresponding left eigenvector. Condition (A.4) serves as a closure condition that identifies admissible shock speeds, D.

Because analytic integration of (A.2) is rarely possible, a numerical procedure is required. When a vanishing eigenvalue exists somewhere in the flow, we need a numerical algorithm to determine the values of D for which (A.4) is satisfied. Importantly, the location of the critical point is unknown *a priori*. A simple approach to solving this problem is to make a guess for D and integrate from $\eta = 0$ up to the singular point, and then check whether or not $\mathbf{l}_* \cdot \mathbf{s}_* = 0$ is satisfied. This is a numerically ill-conditioned procedure since the system becomes stiffer as one approaches the singular point, the latter having a saddle-point nature.

Our integration procedure avoids the numerical problems associated with the presence of a sonic point. The key idea is based on the use of a new dependent variable given by

$$\boldsymbol{z} = \mathbf{G}(\boldsymbol{q}; D) = \mathbf{F}(\boldsymbol{q}) - D\boldsymbol{q}. \tag{A.5}$$

The governing system of ODEs written in terms of $\mathbf{z}$ becomes

$$\boldsymbol{z}_\eta = \mathbf{s}(\boldsymbol{q}), \tag{A.6}$$

and needs to be solved subject to the shock conditions, $\boldsymbol{z}(0) = \mathbf{F}(\boldsymbol{q}_0) - D\boldsymbol{q}_0$, with $\mathbf{q}_0$ denoting the post-shock state. In order for this change of variables to be successful, it must be invertible so that $\boldsymbol{q} = \mathbf{G}^{-1}(\boldsymbol{z}, D)$. The inversion is guaranteed to be well defined as long as the Jacobian, $\mathbf{G_q} = \mathbf{F_q} - D\mathbf{I}$, is not singular, which is the case away from sonic points. It is important to note that, in general, the inversion results in multiple solution branches. In order to choose the correct branch, we need to ensure that $\mathbf{G}^{-1}(\boldsymbol{z}(0)) = \boldsymbol{q}_0$.

The main advantage of the new variable is that (A.6) is not stiff even as one approaches the singular point and

thus the problem of finding the values of D such that (A.4) is satisfied becomes regular. The analytical inversion of $\mathbf{G}$ may not in general be possible as it depends on the specific form of the equation of state. Nevertheless, the general procedure remains valid and, once the sonic points are found, the inversion can be done numerically.

To specialize the previous analysis to one-dimensional reactive Euler equations, we begin with the equations written in conservation form:

$$\rho_t + (\rho u)_x = s_1, \tag{A.7}$$

$$(\rho u)_t + \left(\rho u^2 + p\right)_x = s_2, \tag{A.8}$$

$$(\rho e)_t + (\rho u e + p u)_x = s_3, \tag{A.9}$$

$$(\rho \lambda)_t + (\rho u \lambda)_x = s_4. \tag{A.10}$$

We have chosen to keep $\mathbf{s}$ general for now. It can account for such effects as curvature, heat and momentum losses, area changes, etc. For simplicity, we assume a perfect gas equation of state and therefore $e = pv/(\gamma - 1) - Q\lambda + u^2/2$, $p = \rho RT$, where Q is the heat of reaction, λ is the heat-release progress variable, and R is the universal gas constant. Now, let $q_1 = \rho$, $q_2 = \rho u$, $q_3 = \rho e$, $q_4 = \rho\lambda$. Then, $p = (\gamma - 1)\left(q_3 - \frac{q_2^2}{2q_1} + Qq_4\right)$. In terms of these conserved quantities, we find that

$$\mathbf{F}(\boldsymbol{q}) = \begin{pmatrix} q_2 \\ q_2^2/q_1 + (\gamma - 1)\left(q_3 - \frac{q_2^2}{2q_1} - Qq_4\right) \\ q_2 q_3/q_1 + \frac{q_2}{q_1}(\gamma - 1)\left(q_3 - \frac{q_2^2}{2q_1} - Qq_4\right) \\ \frac{q_2}{q_1} q_4 \end{pmatrix} \tag{A.11}$$

and the eigenvalues of $\mathbf{F_q}$ (which we do not write for brevity) give the well-known characteristic speeds of the Euler equations in the shock-attached frame:

$$\begin{aligned} \lambda_1 &= q_2/q_1 - \sqrt{\frac{-q_1^2\left(q_2^2 - 2q_1q_3 + 2Qq_1q_4\right)(\gamma - 1)\gamma}{2q_1^4}} = u - c - D, \\ \lambda_2 &= q_2/q_1 = u - D, \\ \lambda_3 &= q_2/q_1 = u - D, \\ \lambda_4 &= q_2/q_1 + \sqrt{\frac{-q_1^2\left(q_2^2 - 2q_1q_3 + 2Qq_1q_4\right)(\gamma - 1)\gamma}{2q_1^4}} = u + c - D, \end{aligned}$$

where the sound speed is given by $c = \sqrt{\frac{-\left(q_2^2 - 2q_1 q_3 + 2Qq_1 q_4\right)(\gamma-1)\gamma}{2q_1^2}} = \sqrt{\frac{\gamma p}{\rho}}$. In order to obtain the regularity condition at the sonic point, we need to know the left eigenvector associated with the forward characteristic. It is given by

$$l_4 \;=\; \left(u^2\left(\gamma-1\right) - uc, \quad c - u\left(\gamma-1\right), \quad \left(\gamma-1\right), \quad Q\left(\gamma-1\right)\right).$$

Thus, should there be a sonic point in the flow ($\lambda_4 = 0$), it is necessary that $\mathbf{l}_4 \cdot \mathbf{s}$ should vanish at the sonic point in order for $\boldsymbol{q}_\eta$ to be bounded.

Following the general procedure outlined above, we define

$$\begin{aligned}
z_1 &= q_2 - Dq_1, \\
z_2 &= q_2^2/q_1 + (\gamma-1)\left(q_3 - \frac{q_2^2}{2q_1} - Qq_4\right) - Dq_2, \\
z_3 &= q_2 q_3/q_1 + \frac{q_2}{q_1}(\gamma-1)\left(q_3 - \frac{q_2^2}{2q_1} - Qq_4\right) - Dq_3, \\
z_4 &= \frac{q_2}{q_1} q_4 - Dq_4.
\end{aligned} \tag{A.12}$$

We obtain the inverse, $\boldsymbol{q} = \boldsymbol{q}(z_1, z_2, z_3, z_4)$, as

$$\begin{aligned}
q_2 &= z_1 + Dq_1 \\
q_3 &= \frac{D^2 q_1^2 z_1 + 2Dq_1 z_1^2 + z_1^3 - Dq_1^2 z_2 - q_1 z_1 z_2 + q_1^2 z_3}{q_1 z_1} \\
q_4 &= \frac{q_1 z_4}{z_1}
\end{aligned} \tag{A.13}$$

with

$$q_1 = \frac{\gamma z_1(z_2 - Dz_1) \pm \sqrt{z_1^2\left(D^2 z_1^2 - 2Dz_1 z_2 + \gamma^2 z_2^2 - 2\left(\gamma^2-1\right) z_1(z_3 + Qz_4)\right)}}{D^2 z_1 - 2Dz_2 + 2(\gamma-1)(z_3 + Qz_4)}. \tag{A.14}$$

The choice of the inversion branch depends on which branch of the square root in (A.14) is chosen. We note that the expression under the square root is

$$\delta \;\equiv\; z_1^2\left(D^2 z_1^2 - 2Dz_1 z_2 + \gamma^2 z_2^2 - 2z_1(z_3 + Qz_4)\left(\gamma^2-1\right)\right) = \rho^4 \lambda_1^2 \lambda_3^2 \lambda_4^2, \tag{A.15}$$

i.e., it is a perfect square that vanishes only when one of the eigenvalues of the Jacobian, $\mathbf{F_q} - D\mathbf{I}$, becomes zero.

One can thus simplify q_1 as

$$q_1 = \frac{\rho\left(\gamma(u-D)^2+c^2\right) - \text{sign}(u-D)\rho\left|(u-D+c)\,(u-D-c)\right|}{(\gamma-1)\left((u-D)^2+\frac{2}{\gamma-1}c^2\right)}. \tag{A.16}$$

The correct branch of the transformation is selected by requiring that $\boldsymbol{q}(\boldsymbol{z}(0)) = \boldsymbol{q}(0)$, which can be seen to be the negative branch. Across the sonic point, the solution branch changes.

In order to illustrate the previous calculation with a well-known example, we consider the small curvature approximation of the reactive Euler equations, which can be written in a shock-attached frame as (see, e.g., [24]),

$$\left(\rho\,(u-D)\right)_\eta = -\kappa\rho u, \tag{A.17}$$

$$\left(p+\rho u\,(u-D)\right)_\eta = -\kappa\rho u^2, \tag{A.18}$$

$$\left(\rho\,(u-D)\,e+pu\right)_\eta = -\kappa\left(\rho u e+pu\right), \tag{A.19}$$

$$\left(\rho(u-D)\lambda\right)_\eta = \rho\omega-\kappa\rho u\lambda. \tag{A.20}$$

Here, $\omega=\omega\,(p,\rho,\lambda)$ is a general rate function, not necessarily of Arrhenius form. As before, we define new dependent variables as in (A.12) and the inverse as in (A.13). The system written in terms of the new variable is simply $\boldsymbol{z}_\eta = \mathbf{s}(\boldsymbol{z})$. In this particular case, the total enthalpy, $H=\frac{\gamma p}{(\gamma-1)\rho}+\frac{(u-D)^2}{2}-\lambda Q$, can be shown to be a conserved quantity. Therefore, using the upstream state to rescale the variables with respect to p_a, ρ_a, and $\sqrt{p_a/\rho_a}$, we find that $H=\frac{D^2z_1-2Dz_2+2z_3}{2z_1}=H_0=\frac{\gamma}{\gamma-1}+\frac{D^2}{2}$. Then, we eliminate z_3 in favor of the remaining variables, $z_3=\frac{\gamma}{\gamma-1}z_1+Dz_2$, to arrive at the following system:

$$\left(z_1\right)_\eta = -\kappa q_2, \tag{A.21}$$

$$\left(z_2\right)_\eta = -\kappa\frac{q_2^2}{q_1}, \tag{A.22}$$

$$\left(z_4\right)_\eta = \frac{-\kappa q_2 q_4+\omega}{q_1}, \tag{A.23}$$

which is free from singularity. It should be integrated numerically from the shock to the sonic point with the negative branch in (A.14) and, if necessary, further from the sonic point using the positive branch.